The Sequence Stratigraphic Division and Depositional Environment of the Jurassic Yan'an Formation in the Pengyang Area, Southwestern Margin of the Ordos Basin, China

Lianfu Hai [1,2,3], Caixia Mu [1,2], Qinghai Xu [4,*], Yongliang Sun [1,2], Hongrui Fan [3], Xiangyang Xie [5], Xiangcheng Wei [1,2], Chao Mei [1,2], Haibin Yu [1,2], Walter Manger [6] and Jun Yang [4]

1 Mineral Geological Survey Institute of Ningxia Hui Autonomous Region, Yinchuan 750021, China; hailianfu163@outlook.com (L.H.); caixia.mu@outlook.com (C.M.); sunyongliang134@outlook.com (Y.S.); xiangcheng.wei@outlook.com (X.W.); chao.mei112@outlook.com (C.M.); yuhaibinyhb@outlook.com (H.Y.)
2 Institute of Mineral Geology of Ningxia Hui Autonomous Region, Yinchuan 750021, China
3 Institute of Geology and Geophysics, Chinese Academy of Sciences, Beijing 100029, China; fanhrig@outlook.com
4 School of Geosciences, Yangtze University, Wuhan 430100, China; yangjun1229@outlook.com
5 School of Geology, Energy, and Environment, Texas Christian University, Fort Worth, TX 76129, USA; x.xie@tcu.edu
6 Department of Geosciences, University of Arkansas, Fayetteville, AR 72701, USA; 4795312883@mms.att.net
* Correspondence: qinghai.xu@yangtzeu.edu.cn

Abstract: Coal and organic-rich shale in the Yan'an Formation in the southwestern margin of the Ordos Basin are widely developed, which is an important fact for oil and gas exploration in China that has been widely explored for a long time. In this paper, detailed sequence division and sedimentary environment analyses of the Yan'an Formation in the Pengyang area on the southwestern margin of the Ordos Basin were conducted using field outcrops, drilling cores, logging, wavelet transform and organic geochemistry. The results showed that the succession consists of some units with distinctly different characteristics. Based on the petrographic assemblage and transform wavelet characteristics, the Yan'an Formation in this area can be divided into a long-term cycle, five medium-term cycles, and eleven short-term cycles, among which coal and carbonaceous shale were mainly developed in the short-term cycles I_2, III_1, III_2, V_1 and V_2. Coal and organic-rich mud shale have been developed in the Yan'an Formation and plant debris in mudstone and coal is common, indicating the development of swamps and shallow water-covered depressions in this area. The sandstones showed parallel bedding, cross-bedding and scours, thus indicating fluvial deposits. The saturated hydrocarbon gas chromatographic parameters of mud shale showed that the pristane/phytane (Pr/Ph) ratio is 2.24–6.22, the Ph/nC18 ratio is 0.15–0.93, and the Pr/nC17 ratio is 0.97–2.78, supporting the finding that the organic matter has mainly originated from terrestrial sources.

Keywords: Ordos Basin; Pengyang; Yan'an Formation; sequence classification; peat environment

1. Introduction

The sedimentary cycle is a regular reflection of different geological and historical events in the lithology of strata. Episodic tectonic movements, celestial cycles, and global sea level changes are the main controlling factors for the formation of sedimentary cycles, and the formation of continuous sedimentary strata has a certain periodic rhythm. Therefore, it is important to study the sedimentation cycle level and genesis to deduce the original sedimentation dynamics and main controlling factors. The Jurassic Yan'an Formation formed during the main oil shale and coal forming period [1–4]. The period when the Yan'an Formation developed was also a major stage of basin evolution and the formation of oil and gas [5–8]. Many Jurassic tectonic reservoirs have been discovered in the western margin of the Ordos Basin, among which the Yan'an Formation is the main oil-producing

formation with promising exploration prospects and has become an important region for oil and gas exploration within the Ordos Basin [9–14]. The southwest margin of the Ordos Basin is located at the joint occurrence of geotectonic units of the North China Craton, the Alashan Massif, the Qinling orogenic belt, and the Qilian orogenic belt [14]. Due to the strong influence of the thrust tectonics on the western margin of the basin, the Jurassic was generally subjected to uplift and denudation, resulting in debates about the correct stratigraphic position of the various sedimentary successions. To accurately understand the sedimentary evolution of the Yan'an Formation and to guide oil and gas exploration in the area, the authors of this paper selected the Pengyang area on the southwest margin of the basin as their study area, and they used detailed observations of cores and small wavelet transforms combined with logging data for research. The results may provide basic data for transferring field data to process models for the Yan'an Formation [15].

2. Geological Setting

The Ordos Basin is a superimposed basin formed in the Mesoproterozoic Era above the North China Craton [16–19]. The basement mainly consists of Precambrian metamorphic crystalline rocks of the North China Craton and Middle Paleozoic marine tuffs interbedded with clastic rocks [20]. The overlying formation comprises middle Cenozoic continental clastic rocks [21,22], and the specific stratigraphy is mainly the late Triassic Extension, Jurassic, Cretaceous, Oligocene, Pliocene and Quaternary groups [23]. Internally, the Ordos Basin can be subdivided into six tectonic units: the Yimeng Uplift, the Western Thrust Belt, the Tianhuan Depression, the Yishan Slope, the Jinxi Flexure Belt, and the Weibei Uplift (Figure 1). The Pengyang area is located at the southwest margin of the Ordos Basin, and the geotectonic position is in the southern part of the Tianhuan Depression (Figure 1) adjacent to the Yishan Slope in the east and the margin of the Western Thrust Belt.
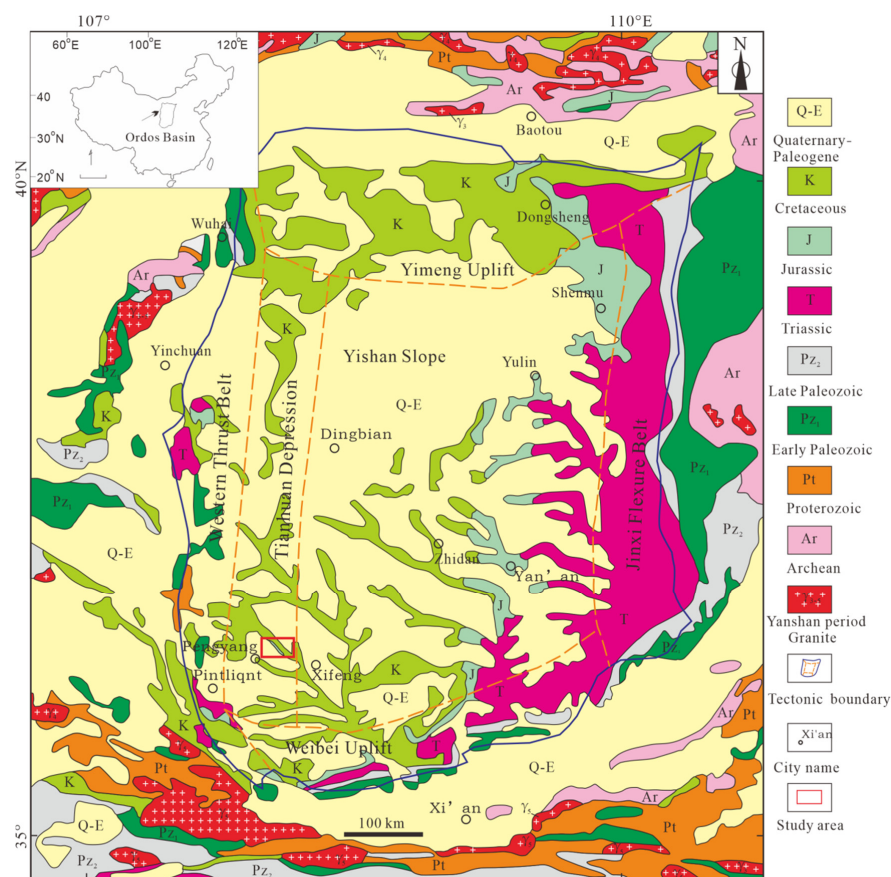
Figure 1. Structural unit and geological map of Ordos Basin (modified from the work of Zhao et al., 2020 [6]).

The topography of the study area is relatively simple, mostly covered by Quaternary deposits, with only sporadic bedrock outcrops in some large gullies. The main strata are the middle Ordovician Pingliang Formation, Lower Ordovician Baota Formation, Middle Jurassic Yan'an Formation, Lower Cretaceous Heshangpu Formation, Lower Cretaceous Liwaxia Formation, Middle Neogene Ganhegou Formation, and the Quaternary strata (Figure 2). The Middle Ordovician Pingliang Formation is dominated by light black and yellow-green thin-layered shales and siltstones, interspersed with fine sandstones and conglomeratic tuffs, and is a set of shallow marine deposits [5,6]. The Lower Ordovician Baota Formation consists of grey or slightly red medium-to-thick-bedded limestone, and it is a set of terrace-phase carbonate deposits [24]. The Jurassic Yan'an Formation is characterized by coal, oil shale, mudstone, and sandstones. The Lower Cretaceous Heshangpu Formation as a whole consists of purplish-red sandy mudstones, muddy sandstones interspersed with light grey-green sandstones and grey muddy sandstones (which are fluvial in origin [25]), while the Liwaxia Formation mainly consists of grey-green and purplish-red mudstones, muddy sandstones, marl and a few fine sandstones that are lacustrine in origin [25]. The Miocene Ganhegou Formation is the top sedimentary stratum of the Neogene, a set of fluvial clastic deposits consisting of sandstone, conglomerate, sandstone, siltstone and silty mudstone [26].
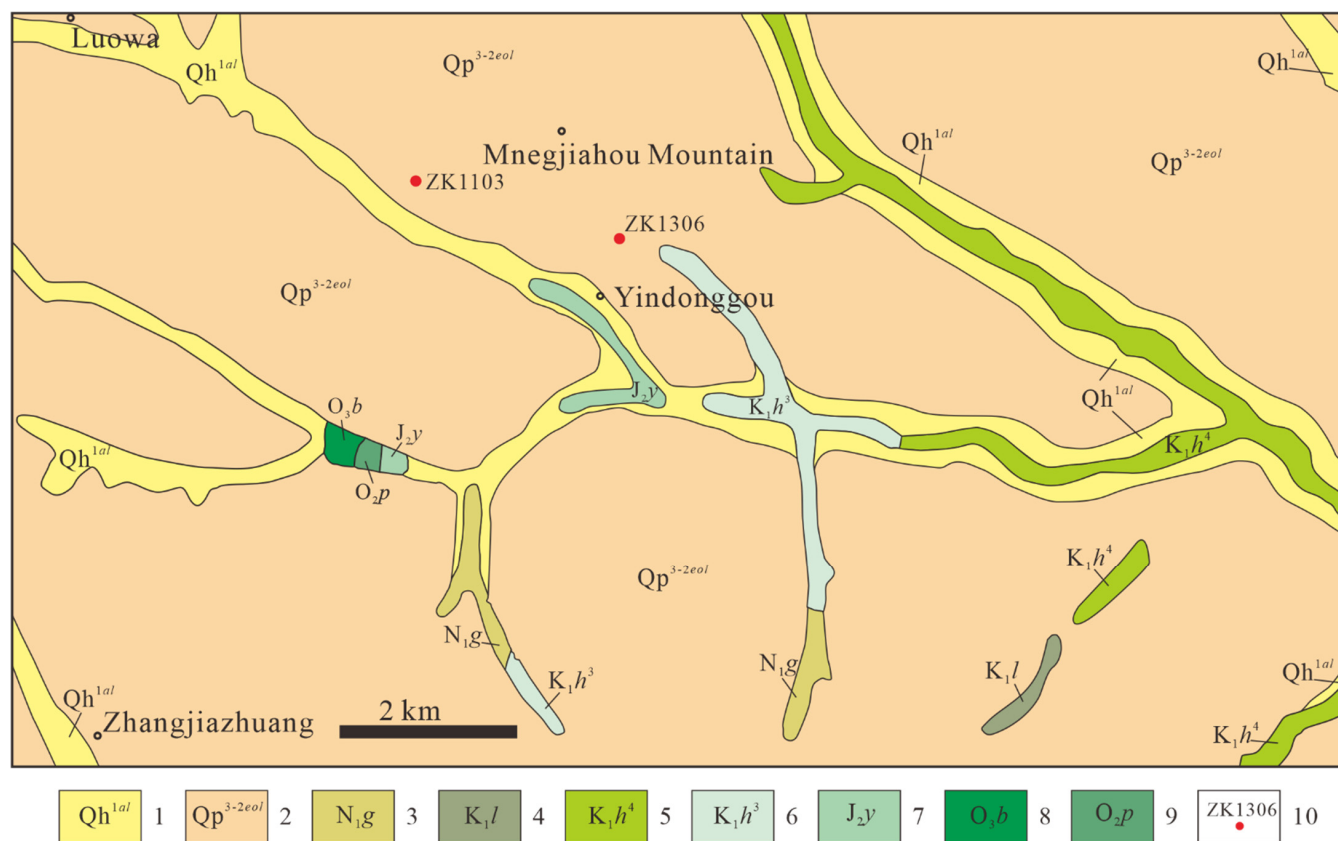
Figure 2. Geological map of Yindonggou Coal Mine in Pengyang area (location in Figure 1). Key: Quaternary Holocene alluvial layers (Qh^{1al}); Quaternary Pleistocene aeolian layers (Qp^{3-2eol}); Ganhegou Formation of Neogene (N_1g); Liwaxia Formation of Cretaceous (K_1l); the fourth lithological member of the Heshangpu Formation of Cretaceous (K_1h^4); the third lithological member of the Heshangpu Formation of Cretaceous (K_1h^3); Yan'an Formation of Jurassic (J_{2y}); Baota Formation of Ordovician (O_3b); and Pingliang Formation of Ordovician (O_2p). ZK1306 is the location and well name.

The Yan'an Formation of the Middle Jurassic is the main coal-bearing stratigraphic unit in the study area. According to the data in published papers, the Yan'an Formation has a large

variation in depositional thickness and lithology and is a sandstone–conglomerate–mudstone assemblage with predominantly fluvial deposits, along with local sections deposited in lake and marsh phases [27–29]. Depending on their lithology and depositional environment, they can be regionally divided into four lithological members. The first lithological member is dominated by lacustrine fine clastic rocks with frequent interactions of light-grey thin-bedded fine sandstone with siltstone and mudstone, and the lithological assemblage is more distinctive, showing grey and black bands throughout the member. The second lithological member is dominated by brownish-red, thick-bedded, coarse-grained feldspathic quartz sandstone in the lower part of the section and by lacustrine fine clastic rocks in the middle and upper parts, with thinly interbedded siltstone, mudstone, and fine sandstone. The third lithological member is dominated by coarse clastic rocks, with thick grey-white bedded feldspar or feldspathic quartz sandstone layers interbedded with thin coal seams. There is grey-white, slightly yellowish-green, coarse-to-medium-grained sandstone at the bottom; sandstone layers in the middle section; and coarse sandstone layers in the upper section. The fourth lithological member is dominated by grey-red thickly bedded medium-to-coarse-grained iron-bearing feldspar quartz sandstone interbedded with light-grey and grey-red medium-grained feldspathic quartz sandstone, greenish grey siltstone, mudstone, and thin coal-bearing lines.

3. Data and Methodology

In this paper, based on the cores and logging data from borehole ZK1306 collected by the Institute of Mineral Geology of Ningxia Hui Autonomous Region in 2021 at the Yin-donggou coal mine in the Pengyang area, the natural gamma ray (GR) logging parameters of the well were continuously wavelet-transformed based on Morlet wavelets to delineate the stratigraphic sequence of the Yan'an Formation in the study area.

The chronostratigraphic division results of well ZK1306 were provided by the Institute of Mineral Geology of Ningxia Hui Autonomous Region (Figure 3). The depth of borehole ZK1306 is 1011.35 m, of which the section from 1011.35 m to 986.30 m is the Triassic Shangtian Formation. The section from 986.30 m to 688.10 m is the Jurassic Yan'an Formation. The Jurassic Yan'an Formation is the coal-bearing stratum in the area, and a total of seven coal seams were seen in hole ZK1306 (Figure 4). The section between 688.10 m and 602.41 m is the Jurassic Zhiluo Formation, that between 602.41 m and 249.00 m is the Jurassic Anding Formation, that between 249.00 m and 104.55 m is the Cretaceous Yijun Formation, and that between 104.55 m and 0 m is the Paleogene and Quaternary.
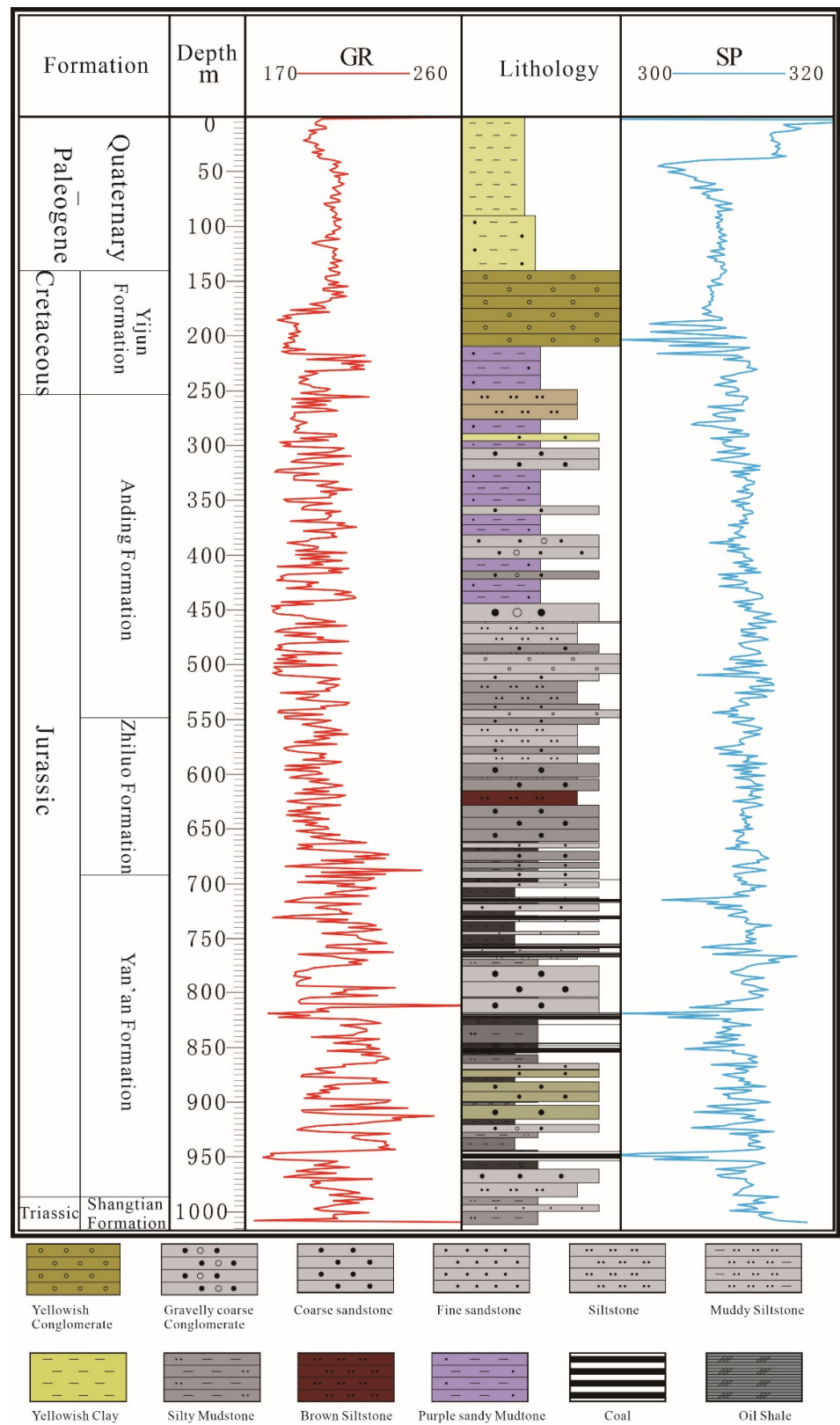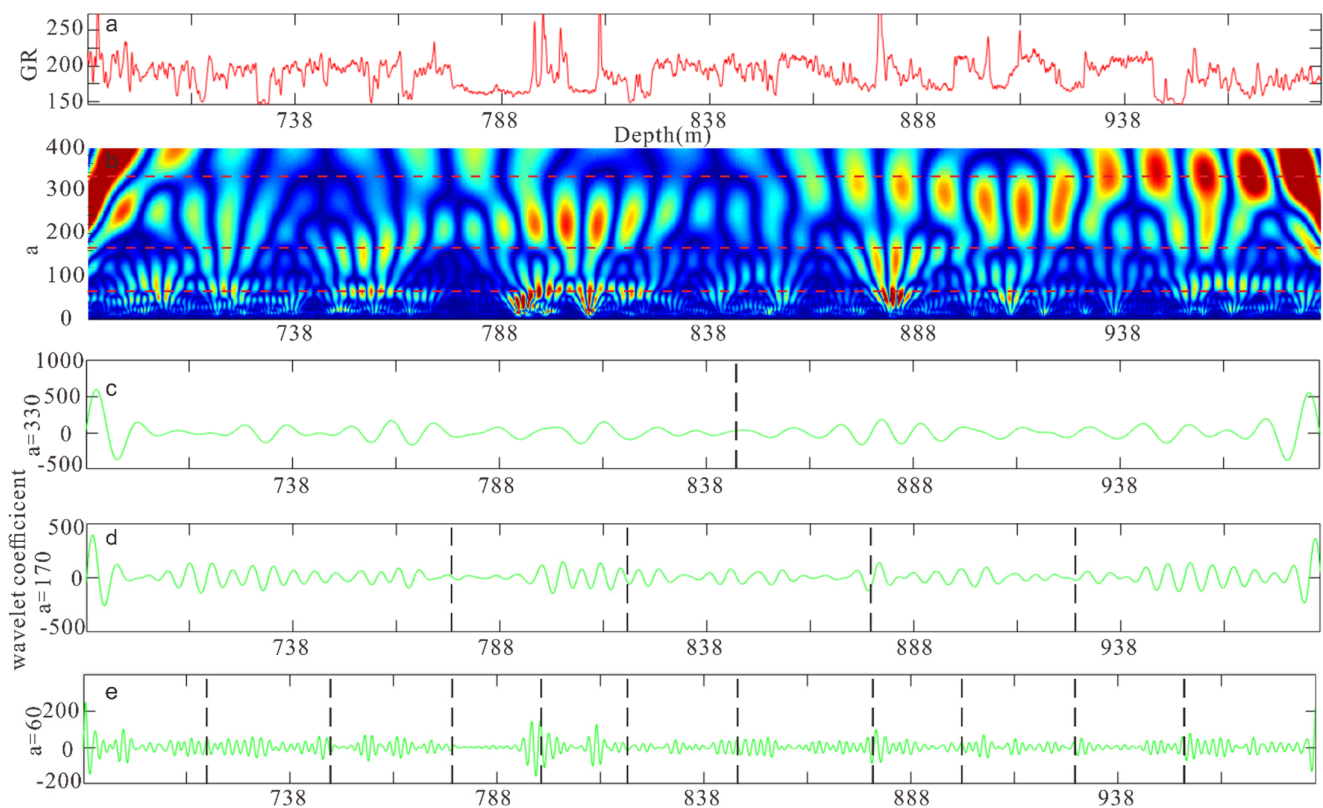
Figure 3. The stratigraphic column of the well ZK1306.

Figure 4. The continuous wavelet transform of gamma rays. (**a**) The gamma ray logging curve of Yan'an Formation of well ZK1306; (**b**) time−frequency chromatogram of wavelet-transform coefficient; (**c**) the curve of wavelet transforms with a scale of 330; (**d**) the curve of wavelet transforms with a scale of 170; and (**e**) the curve of wavelet transforms with a scale of 60. The red dashed line indicates the average value of scale a that could be used to identify the cycles.

4. Results

4.1. Delineation of the Yan'an Formation Stratigraphy

Based on the lithologies, the Yan'an Formation can be divided into five sublayers (Table 1). From 927.40 m to 986.30 m, a thick layer of siltstone and fine sandstone developed in the lower part and carbonaceous mudstone and coal seam developed in the upper part; from 877.50 m to 927.40 m, a gravelly coarse sandstone developed at the bottom and a thick layer of grey-green and grey medium sandstone with thin mudstone developed in the middle and upper parts; and from 818.14 m to 877.50 m, a set of fine sandstones developed at the base, becoming mudstone and coarse sandstone upwards, with thick layers of siltstone, coal seam and carbonaceous mudstone in the middle and upper parts. From 775.77 m to 818.14 m, thick layers of coarse sandstone developed in the upper and lower parts, with fine sandstone and carbonaceous mudstone in the middle part. The black mudstone and coal seam developed, interspersed with thin layers of fine sandstone, from 688.10~775.77 m. A layer of coarse sandstone was found to be present in the upper part (Figure 4).

The wavelet-transform technique was used to extract the stratigraphic development features hidden in the original logging data, thus more obviously reflecting the trend changes of the sedimentary cycles within the strata. Furthermore, the stratigraphic interface could be determined and the cycles could be classified to meet the requirements of high-resolution stratigraphic delineation by analyzing the trend patterns of different levels of curves [30]. The wavelet transform was used to convert the one-dimensional depth-domain logging data information into two-dimensional depth (b) and scale (a) domain time–frequency information. Therefore, the information of different levels of sedimentary

cyclotrons superimposed in the logging data was decomposed into respective period-independent sedimentary spins by the wavelet transform and presented in the form of scale (a) [31–34]. The larger the scale (a), the narrower the frequency band and the lower the resolution, corresponding to the long-period component of the signal and indicating long depositional cycles and large stratigraphic thickness that can be used to classify long-period cyclones [34,35]. The smaller scale (a), the wider frequency band and the higher resolution, corresponding to the short-period component of the signal and indicating short depositional cycles and small stratigraphic thickness that can be used to classify medium-, short-, and ultrashort-period cyclones [34,35].

Table 1. The lithologies of Yan'an Formation drilled by well ZK1306.

Formation	Sublayer	Bottom (m)	Top (m)	Lithology
Yan'an Formation	Y_5	775.77	688.10	Mudstone, coal seam, fine sandstone, and coarse sandstone
	Y_4	818.14	775.77	Coarse sandstone, fine sandstone, and carbonaceous mudstone
	Y_3	877.50	818.14	fine sandstone, coarse sandstone, Mudstone, siltstone, coal seam, and carbonaceous mudstone
	Y_2	927.40	877.50	Gravelly coarse sandstone, medium sandstone, and mudstone
	Y_1	986.30	927.40	Siltstone, fine sandstone, carbonaceous mudstone

The natural gamma ray logging curve of well ZK1306 at depths from 985.53 m to 688.10 m (Yan'an Formation), with a sampling interval of 0.05 m and GR values ranging from 176.54 to 278.44 API, is shown in Figure 4a. Figure 4b shows the time–frequency chromatogram of wavelet coefficients obtained by the Morlet wavelet transform of the GR curve, with blue-green to yellow-red representing wavelet coefficients from low to high values, respectively. It can be seen that in the scale range from 280 to 380 (average = 330, read dashed line), the colour change has obvious two-stage characteristics, mainly showing a large-scale sedimentary cycle. Therefore, the curve of wavelet transforms with a scale of 330 could be used to classify a long-term cycle. The 330 scale wavelet-transform coefficient curve and spectrograms show clear boundaries at a depth of 838.80 m, which divides the Yan'an Group into two sections (Figure 4c). There are obvious cyclic changes at a scale range from 120 to 220 (average = 170), which could be used to classify medium-term cyclogenesis (Figure 4b). Therefore, the curve of wavelet transforms with a scale of 170 could be used to classify middle-term cycles (Figure 4d). Additionally, the scale ranges from 50 to 170 were found to have more high-resolution cycles (average = 60). Therefore, the curve of wavelet transforms with a scale of 60 could be considered to correspond to high frequency stratigraphic cycles, which could be used to classify short-term cycles.

The average value of the three scale ranges was chosen and the wavelet-transform coefficient curves were obtained with MATLAB for scales of 330, 170 and 60 to identify the sediment cycles (Figure 4). The lithology also showed that the Yan'an Formation has a generally positive spin from 985.53 m to 838.80 m and is generally anticyclonic from 838.80 m to 688.10 m, with the Yan'an Formation having complete positive and negative spin. There are four distinct boundaries on the wavelet-transform coefficient curve and spectrogram at a scale of 170, i.e., at 927.40 m, 877.50 m, 818.14 m, and 775.77 m, dividing the Yan'an Formation into five sections, i.e., five intermediate spins (I−V, Figure 5). The wavelet-transform curves at a scale of 60 showed higher precision variations, further dividing the Yan'an Formation into 11 short-term cycles (Figure 5). The long-term cycle was influenced by regional tectonic movements, and the Indo−Chinese movement at the end of the Triassic caused the uplift of the whole basin [36]. Then, the study area experienced a cyclical process of uplift and subsidence from the beginning of the crust to stabilization and then uplift again during the deposition of the whole Yan'an Formation; hence, the

Yan'an Formation in the study area is classified as a long-term cyclogenesis. The middle-term cycle represents a more complete progradation and recession process, mainly in the form of changes in the depositional environment [34,37]. The sedimentary evolution of the Yan'an Formation in the study area is characterized by five distinct progradation and recession processes, and it can therefore be divided into five medium-term cycles. Short-term cyclogenesis mainly relies on the petrographic assemblage and changes in the phase sequence [34,37,38]. The coarse sandstone, medium sandstone, fine sandstone, mudstone and coal seams were mainly developed during the deposition of the Yan'an Formation in the study area, and the 11 short-term cyclogenetic cycles represent the changes in the petrographic assemblage from coarse sandstone to mudstone and coal seams and then to sandstone. In summary, based on the lithology, electrical properties, and wavelet-transform curves and spectrograms, the Yan'an Formation could be divided into one long-term, five medium-term, and eleven short-term cycles (Figure 5).
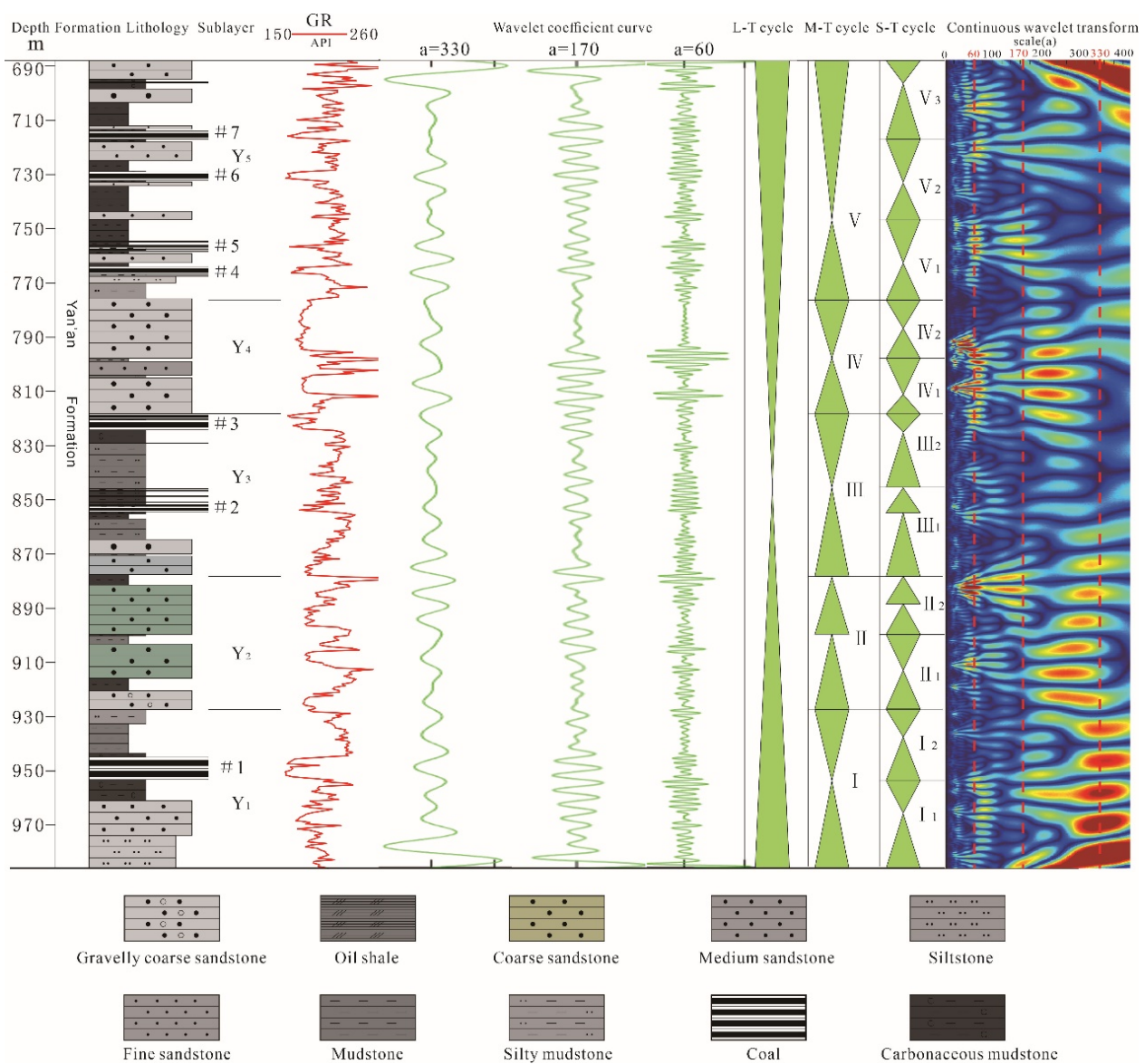

Figure 5. Stratigraphy and geophysical characterstics of the Yan'an Formation in well ZK1306. Key: Cal seam number (#1~#7); long−term cycle (L–T cycle); middle-term cycle (M–T cycle); short-term cycle (S–T cycle); gamma ray (GR).

4.2. Depositional Environments of the Yan'an Formation

Field outcrops showed that the Yan'an Formation in the study area mainly comprises grey-white gravelly coarse sandstone, medium sandstone, fine sandstone, carbonaceous mudstone, mud shale and coal seams. The sandstones are dominated by parallel laminations (Figure 6A), massive laminations (Figure 6B), cross-bedding and scour surfaces (Figure 6C), which are typical of fluvial sedimentary sand bodies. Horizontal laminations were developed in the muddy siltstone (Figure 6D), and coal seams were commonly developed in the grey and grey-black mudstone in the field outcrop, with large variations in coal seam thickness, short lateral extensions of thin coal seams or coal lines (Figure 6E,F), and longer lateral extensions of thick coal seams. Grey and grey-black mudstone were found to dominate the core of drill hole ZK1306, and carbonaceous mudstone and coal were also developed, with large amounts of plant debris developing in the mudstone and coal (Figure 7), thus indicating that the depositional environment was a reducing environment of swamps.
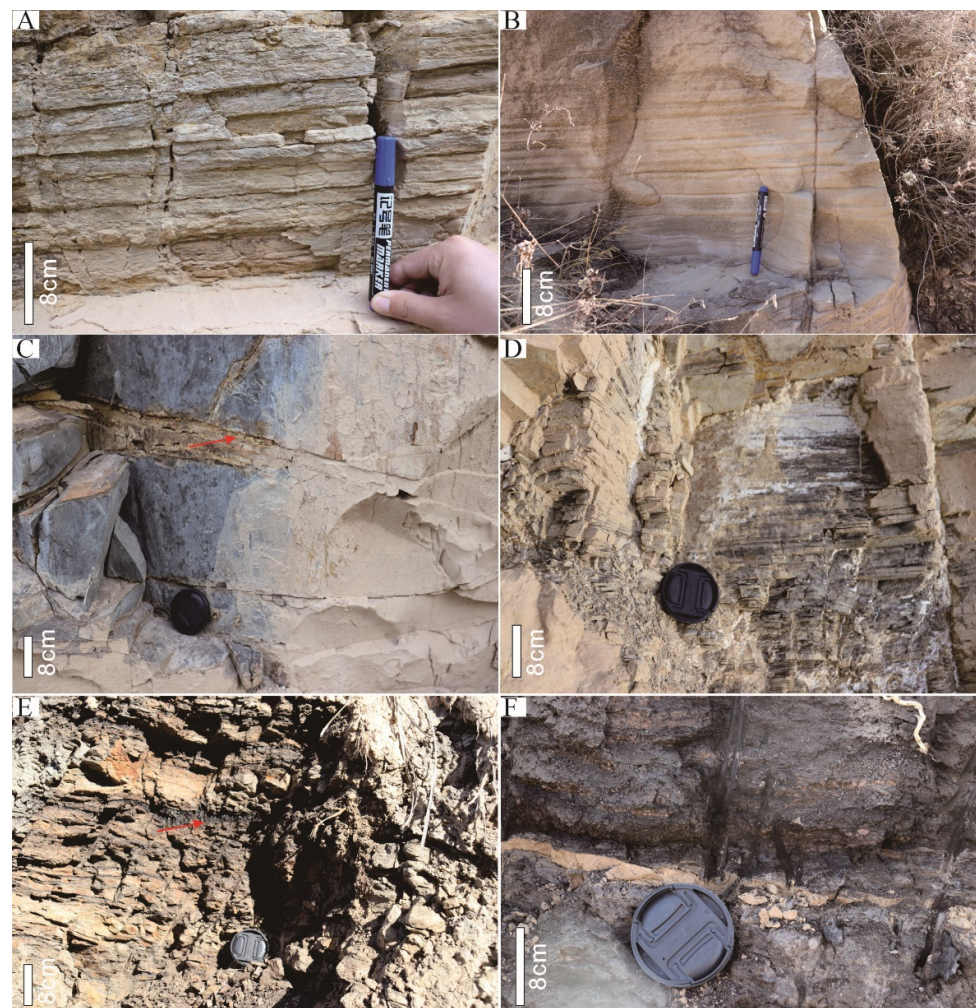
Figure 6. Typical field outcrop profile of Yan'an Formation in Pengyang area. (**A**) Thin-layered fine sandstone intercalated with mudstone in parallel bedding; (**B**) thick massive bedding fine sandstone; (**C**) cross-bedding with scour surface structure (red arrow); (**D**) horizontally bedded argillaceous siltstone; (**E**) coal line (red arrow) that is thick in the middle and gradually pinches out to both sides; and (**F**) grey-black mudstone with coal line, where the coal line is thinned to the left.
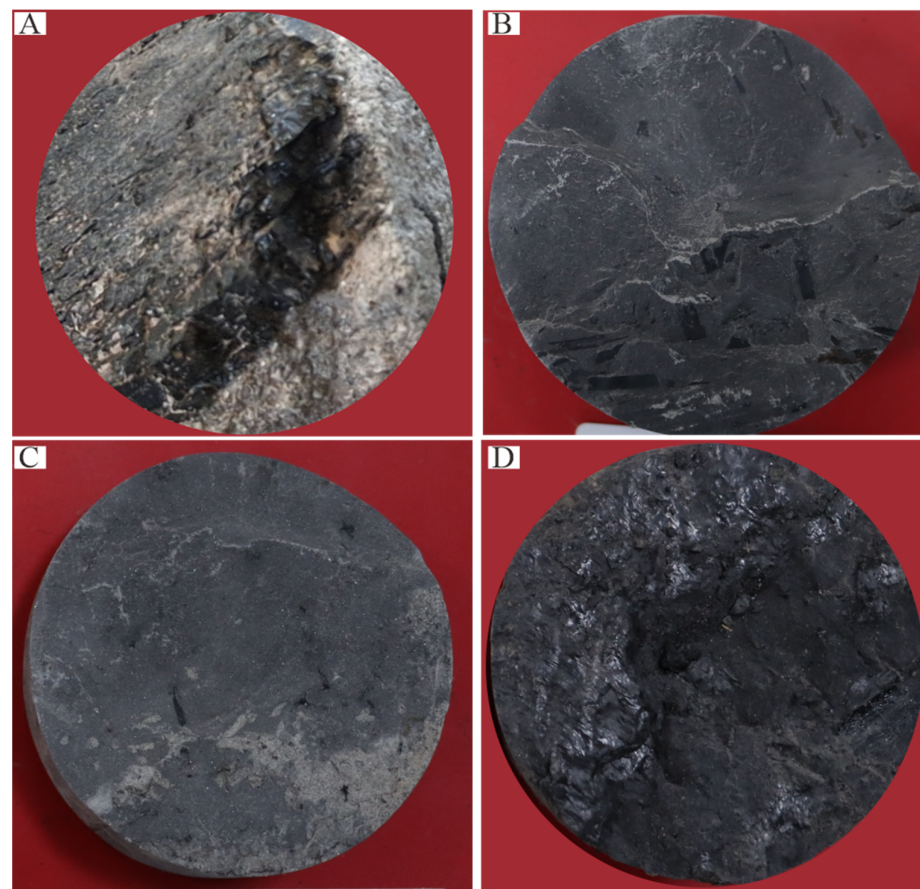
Figure 7. Typical core photos of ZK1306. (**A**) Coarse sandstone, carbonaceous mudstone at the bottom with developed scour surface, 868.4 m; (**B**) grey-black mud shale showing carbonized plant debris development, 845.39 m; (**C**) grey mud shale containing a small amount of plant debris, 716.5 m; and (**D**) black carbonaceous mudstone with coal line, 692.8 m.

5. Discussion

To further define the depositional environment of the Yan'an Formation in the Pengyang area, saturated hydrocarbon gas chromatography analysis was carried out on the mud shale from borehole ZK1306. The samples were mainly collected from the carbonaceous mud shale and coal of the Yan'an Formation, with a depth from 694.90 m to 959.40 m at the base plate. Based on the GB/T 18606-2001 standard as the basis for the detection, saturated hydrocarbon chromatography analysis was performed [38]. The test results are detailed in Table 2.

Table 2. Gas chromatographic parameters of saturated hydrocarbons in shale of Yan'an Formation in Pengyang area.

Sample Number	Lithology	Depth/m	N-alkyl Hydrocarbons				Isoprenoid Alkanes		
			$n\text{-}C_{17}$/%	$n\text{-}C_{18}$/%	Pr/%	Ph/%	Pr/Ph	Pr/$n\text{-}C_{17}$	Ph/$n\text{-}C_{18}$
zk1	Shale	693.9	1.14	1.77	1.11	0.33	3.36	0.97	0.19
zk10	Coal	848.3	1.08	1.75	2.05	0.54	3.77	1.91	0.31
zk15	Shale	952.6	1.66	2.72	1.69	0.42	4.05	1.02	0.15
zk2	Coal	716.0	2.20	2.46	5.10	2.28	2.24	2.32	0.93
zk4	Shale	731.0	1.50	1.95	4.17	0.62	6.22	2.78	0.34
zk16	Shale	959.4	1.17	1.89	2.02	0.37	5.46	1.73	0.20

The results showed that the n-C_{17} mass fraction of the six samples ranged from 1.08% to 2.20%, with an average of 1.46%; the nC_{18} mass fraction ranged from 1.75% to 2.72%, with an average of 2.09%; the Pr mass fraction ranged from 1.11% to 5.10%, with an average of 2.69%; and the Ph mass fraction ranged from 0.33% to 2.28%, with an average of 0.76%. The distribution of Pr/Ph values ranged from 2.24 to 6.22, Ph/nC_{18} values ranged from 0.15 to 0.93, and Pr/n-C_{17} values ranged from 0.97 to 2.78. It is evident from the point-to-point geochemical characteristics map (Figure 8) that the organic matter in the Yan'an Formation mud shale of the Pengyang area was derived from a continental environment, further demonstrating the lack of lake development in the area [39]. The western margin of the basin, i.e., the neighboring area, was tectonically stable during the deposition of the Yan'an Formation when the basin was part of the Craton depression basin and the basin basement was high in the west and low in the east, leading to the flow direction of ancient rivers from west to east. Delta deposits developed in the Huanxian and Qingyang areas on the southwestern margin of the basin, rivers and swamps mainly developed in the western part of the study area, and lake deposits developed in the east (Figure 9).
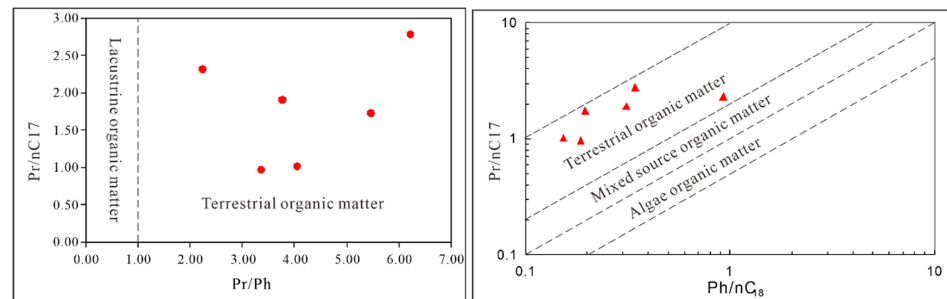
Figure 8. Organic geochemical characteristics of shale in Yan'an Formation (on the basis of the work of Shanmugam, 1985 [39]).
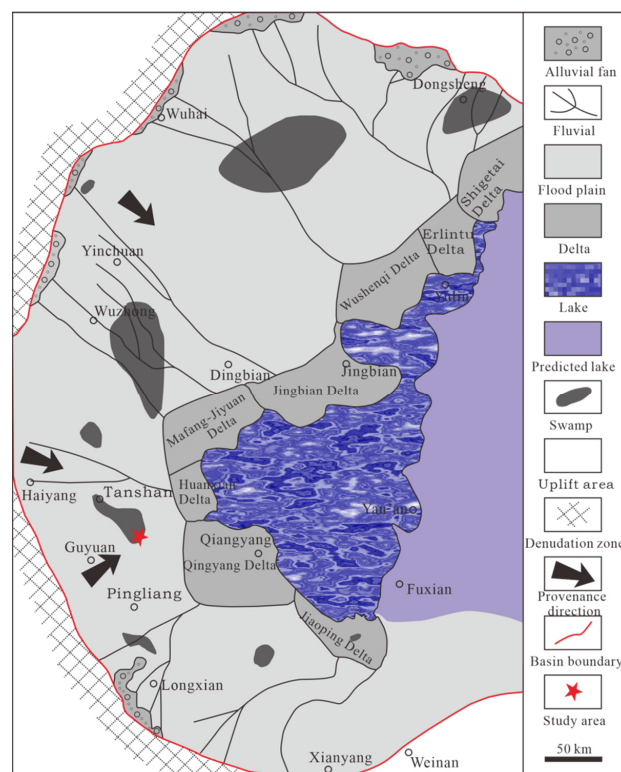
Figure 9. The sedimentary environment and paleogeography of the Jurassic in the western Ordos Basin (modified after Zhang, 2010 [40]).

In summary, the Yan'an Formation in the Pengyang area of the southwestern margin of the Ordos Basin mainly developed swamps and fluvial deposits during the Jurassic.

6. Conclusions

The stratigraphic delineation and sedimentary environment analysis of the Yan'an Formation in the Pengyang area of the southwestern margin of the Ordos Basin led to the following main conclusions.

(1) The Middle Jurassic Yan'an Formation is the main coal-bearing formation in the Pengyang area at the southwest margin of the Ordos Basin. Its lithology and petrographic assemblage are highly variable, with obvious segmentation (mainly in five sections). Wavelet transform was used to divide the Yan'an Formation in this area into a long−term cycle, five medium-term cycles, and eleven short-term cycles.

(2) Coal and organic-rich shale were developed in the Yan'an Formation and plant debris was found to be common in the mudstone and coal, indicating the development of swamps in the area. The sandstones developed parallel laminations, interlaminated laminations, and scour surface structures, which are typical of fluvial deposits.

(3) The mudstones were found to be grey and grey-black in color, and the organic geochemistry analysis of Pr/Ph, Pr/n-C17, and Ph/nC_{18} values indicated that the organic matter is of terrestrial origin, suggesting that the Yan'an Formation was deposited in swamps rather than a lacustrine environment.

Author Contributions: Conceptualization, L.H. and Q.X.; Data curation, Q.X. and C.M. (Chao Mei); Formal analysis, H.F.; Funding acquisition, C.M. (Caixia Mu) and Q.X.; Investigation, X.X. and X.W.; Methodology, C.M. (Chao Mei); Project administration, C.M. (Caixia Mu) and Y.S.; Resources, H.Y.; Software, Q.X. and J.Y.; Supervision, L.H.; Validation, Y.S.; Visualization, X.W.; Writing—original draft, L.H. and Q.X.; Writing—review and editing, X.X. and W.M. All authors have read and agreed to the published version of the manuscript.

Institutional Review Board Statement: Not applicable.

Informed Consent Statement: Not applicable.

Data Availability Statement: Not applicable.

References

1. Han, D.; Yang, Q. *Coalfield Geology in China*; China Coal Industry Publishing House: Beijing, China, 1980.
2. Shi, Z.; Ma, J.; Gao, Z.; Zhang, J.; Liu, K.; Zhao, C. Mineralogical of the Jurassic coals in the middle of Ningdong Coalfield. *J. China Coal Soc.* **2017**, *42*, 1535–1543.
3. Zhang, Z.; Wang, T.; Ramezani, J.; Lv, D.; Wang, C. Climate forcing of terrestrial carbon sink during the Middle Jurassic greenhouse climate: Chronostratigraphic analysis of the Yan'an Formation, Ordos Basin, North China. *GSA Bull.* **2021**, *133*, 1723–1733. [CrossRef]
4. Tang, J.; Tang, S. Single well numerical simulation of middle Jurassic Yan'an Formation Coal No. 2 buried, thermal and hydrocarbon generation history evolution process in coalmine No. 1, Huangling Mining Area. *Coal Geol. China* **2021**, *33*, 32–37.
5. Wang, D.; Shao, L.; Li, Z.; Li, M.; Lv, D.; Liu, H. Hydrocarbon generation characteristics, reserving performance and preservation conditions of continental coal measure shale gas: A case study of Mid-Jurassic shale gas in the Yan'an Formation, Ordos Basin. *J. Pet. Sci. Eng.* **2016**, *145*, 609–628. [CrossRef]
6. Zhao, H.; Dang, B.; Dang, Y.; Wang, X.; Wu, N.; Yang, X.; Wang, Y. Depositional system and its evolution of the Lower Yan'an Formation Jurassic in Ansai district, Ordos Basin. *J. Northwest Univ.* **2020**, *50*, 490–500.
7. Li, Y.; Dai, B.; Huai, H.; Cao, L.; Gao, D.; Xu, Z.; Niu, H.; Hou, T.; Liu, N.; Fan, D. Paleomorphology of Jurassic in the southern area of Ansai Oilfield and its relationship with oil and gas accumulation in Yan'an Formation. *J. Guilin Univ. Technol.* **2020**, *40*, 486–493.
8. Zhang, N.; Xu, Y.; Qiao, J.; Ning, S. Organic geochemistry of the Jurassic tar-rich coal in Northern Shaanxi Province. *Coal Geol. Explor.* **2021**, *49*, 42–49.

9.   Guo, H.; Shi, Y.; Wang, C.; Zhang, S.; Li, W.; Zhong, J. Saturation distribution and log interpretation method of low-contrast reservoir in Mesozoic Yan'an Formation of Ordos Basin. *Well Logging Technol.* **2016**, *40*, 556–563.

10. Wang, L.; Chen, P.; Sun, F.; Wang, X.; Li, J. Geochemical characteristics of crude oil from Yanchang and Yan'an Formation in Pengyang area of Ordos Basin and their implications for oil-source. *Mar. Geol. Front.* **2019**, *35*, 49–54+80.

11. Meng, K.; Jin, M.; Wu, B. Jurassic Yan'an Formation reservoir rocks in the Maling oil field, Ordos Basin. *Sediment. Geol. Tethyan Geol.* **2019**, *39*, 73–83.

12. Hai, L.; Wang, L.; Ma, Z.; Xu, Q.; Song, Y.; Bai, J. Oil Shale Characteristics and Sedimentary Environments of the Yan'an Formation in the Middle Jurassic in Tanshan Area, Guyuan, Ningxia. *J. Jilin Univ.* **2020**, *50*, 747–756.

13. Zheng, D.; Wang, Z.; Wang, L.; Huang, H. Low-amplitude structures and its control on hydrocarbon enrichment and accumulation: An example from Yan'an Formation in Pengyang Area, Ordos Basin. *Geoscience* **2021**, *35*, 1114–1123.

14. Mudunuru, M.K.; Carey, J.W.; Chen, L.; Kang, Q.; Karra, S.; Vesselinov, V.V.; Middleton, R.S.; Johnson, P.A.; Viswanathan, H.S. Subsurface energy: Flow and reactive-transport in porous and fractured media. In *Handbook of Porous Materials: Synthesis, Properties, Modeling and Key Applications Volume 4-Porous Materials for Energy Conversion and Storage*; Eisenberg, E., Ed.; World Scientific: Singapore, 2021; pp. 323–395.

15. Pan, G.; Lu, S.; Xiao, Q.; Zhang, K.; Yin, F.; Hao, G.; Luo, M.; Ren, F.; Yuan, S. Division of tectonic stages and tectonic evolution in China. *Earth Sci. Front.* **2016**, *23*, 1–2.

16. Wang, X.; Liu, Y.; Hou, J.; Li, S.; Kang, Q.; Sun, S.; Ji, L.; Sun, J.; Ma, R. The relationship between synsedimentary fault activity and reservoir quality—A case study of the Ek1 formation in the Wang Guantun area, China. *Interpretation* **2020**, *8*, SM15–SM24. [CrossRef]

17. Deng, J.; Wang, Q.; Gao, B.; Huang, D.; Yang, L.; Xu, H.; Zhou, Y. Evolution of Ordos Basin and its distribution of various energy resource. *Geoscience* **2005**, *19*, 538–545.

18. Liu, C.; Zhao, H.; Wang, F.; Chen, H. Attributes of the Mesozoic structure on the west margin of the Ordos Basin. *Acta Geol. Sin.* **2005**, *79*, 733–747.

19. Liu, C.; Zhao, H.; Gui, X.; Yue, L.; Zhao, J.; Wang, J. Space-time coordinate of the evolution and reformation and mineralization response in Ordos Basin. *Acta Geol. Sin.* **2006**, *80*, 617–638.

20. Yang, X.M.; Ling, M.; Lai, X.; Sun, W.; Liu, C. Uranium Mineral Occurrence of Sandstone–Type Uranium Deposits in the Dongsheng-Huanglong Region, Ordos Basin. *Acta Geol. Sin.* **2009**, *83*, 1167–1177.

21. Ye, J.; Lu, M. Geochemistry modeling of cratonic basin: A case study of the Ordos basin, NW China. *J. Pet. Geol.* **1997**, *20*, 347–362.

22. Zhang, Q.; Li, W.; Liu, W.; Li, Z.; Bai, J.; Yang, B. Jurassic sedimentary system and paleogeographic evolution of Ordos Basin. *Chin. J. Geol.* **2021**, *56*, 1106–1119.

23. Zhao, H.; Li, J.; Miao, P.; Chen, L.; Zhang, B.; Zhu, Q.; Si, Q.; Chen, Y.; Hu, Y.; Guo, H. Mineralogical study of Pengyang uranium deposit and its significance of regional mineral exploration in Southwestern Ordos Basin. *Geotecton. Metallog.* **2020**, *44*, 607–618.

24. Xu, X.; Wan, F.; Yin, F.; Chen, M. Environment facies, ecological facies and diagenetic facies of Baota Formation of Late Ordovina. *J. Mineral. Petrol.* **2001**, *21*, 64–68.

25. Dai, S.; Huang, Y.; Zhao, J.; Zhu, Q.; Liu, J.; Kong, L.; Zhang, M.; Hu, H. The climate change during 128.11–119.05 Ma recorded by the susceptibility of the sediments of Liupanshan Group. *Earth Sci. Front.* **2010**, *17*, 242–249.

26. Li, M.; Li, L.; Liang, Z. Geochemical characteristics and their significances of the Paleogene-Neogene rocks in the Tongxin area, Ningxia, China. *Bull. Miner. Petrol. Geochem.* **2020**, *39*, 304–318.

27. He, W.; Wang, J.; Hai, L.; Wang, L.; Zhao, Y.; Ding, W. Elemental geochemical features of argillaceous rock in Tanshan area Yan'an Formation lower part—A case study of well GY-1. *Coal Geol. China* **2019**, *31*, 7–14.

28. Hai, L.; Xu, Q.; Mu, C.; Tao, R.; Wang, L.; Bai, J. Geochemical characteristics and geologic significance of rare earth elements in oil shale of the Yan'an Formation in the Tanshan area, in the Liupanshan Basin, China. *Interpretation* **2021**, *9*, 843–854. [CrossRef]

29. Zhao, B.; Li, Z.; Gao, C.; Tang, Y. Identification of Complex Fluid Properties in Condensate Gas Reservoirs Based on Gas-Oil Ratio Parameters Calculated by Optimization Mathematical Model. *Front. Energy Res.* **2022**, *10*, 863776. [CrossRef]

30. Zhou, Y.; Du, Y.; Xie, J.; Guo, F.; Zhang, S. Application and comparison of INPEFA technique and wavelet transform in sequence stratigraphic division: A case study in the third member of Dongying Formation in Dawangzhuang area, Raoyang Sag. *China Sci.* **2021**, *16*, 494–501.

31. Li, X. Research on the Application of Multiscale Analysis Method of Well Logging to Sequence Stratigraphy. Ph.D. Thesis, China University Petroleum, Qingdao, China, 2007.

32. Wang, Y.H.; Zhao, P.X.; Zuo, Q.M.; Zhong, Z.H.; Li, J.L. An application of the wavelet transformation to sequence stratigraphy: A case study of the Huangliu Formation in the Yinggehai Basin, northern South China Sea. *Sed. Geol. Teth. Geol.* **2011**, *31*, 58–63.

33. Xun, Z.; Yu, J.; Zhang, X.; Qin, S.; Tian, W. Application of Wavelet Transform in High-Resolution Sequence Stratigraphic Classification. *Shandong Land Resour.* **2017**, *33*, 77–81.

34. Xie, G.; Zheng, J. Cycle division based on matlab wavelet analysis and its geologic implication: A case study of Pinghu Formation in Pb-1 Well of Pingbei section in Baojiao Slope Belt of Xihu sag, Donghai Basin. *Xinjiang Pet. Geol.* **2016**, *37*, 169–172.

35. Zhu, J.B.; Ji, Y.L.; Zhao, P.K.; Wang, Y.H. Application of wavelet transform in auto-identify units of stratigraphy sequence. *Pet. Explor. Dev.* **2005**, *32*, 84–86.

36. Ding, X.; Zhang, S. Sequence stratigraphy analysis of Yan'an Formation in the southwest of Ordos Basin, China. *J. Chengdu Univ. Technol.* **2008**, *35*, 681–685.

37. Li, J.T.; Yu, J.F.; Li, Z.X. The demarcating of stratigraphic sequence based on wavelet transform of well-logging data. *Coal Geol. Explor.* **2004**, *32*, 48–50.

38. *GB/T 18606-2001*; The Standard Text Method for Biomarker in Sediment and Crude Oil by GC-MS. National Standards of the People's Republic of China: Beijing, China, 2001.

39. Shanmugam, G. Significance of Coniferous Rain Forests and Related Organic Matter in Generating Commercial Quantities of Oil, Gippsland Basin, Australia. *AAPG Bull.* **1985**, *69*, 1241–1254. [CrossRef]

40. Zhang, C. Restoration of the Yan'an Period of Jurassic Basin in the Western Margin and Adjacent Areas of Orsos Basin. Master's Thesis, Xi'an Northwest University, Xi'an, China, 2010; pp. 55–56.